Nanoscale

Accepted Manuscript

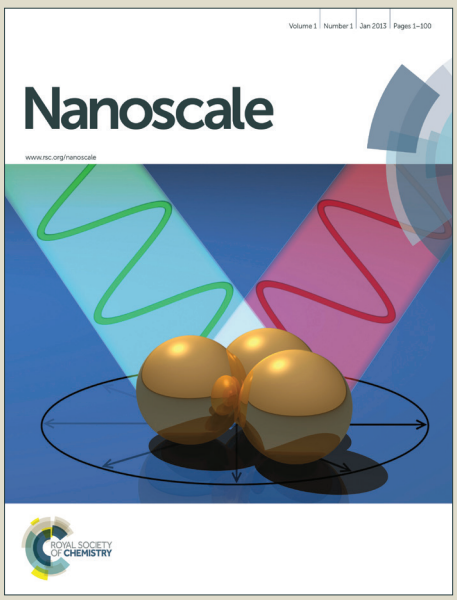

ROYAL SOCIETY OF CHEMISTRY

www.rsc.org/nanoscale

Nanoscale

RSCPublishing

ARTICLE

The Ultimate Step Towards a Tailored Engineering of Core@Shell and Core@Shell@Shell Nanoparticles

Cite this: DOI: 10.1039/x0xx00000x

D. Llamosa[a], M. Ruano[a], L. Martínez[a], A. Mayoral[b], E. Roman[a], M. García-Hernández[a] and Y. Huttel[a]

Received 00th June 2014,
Accepted 00th June 2014

DOI: 10.1039/x0xx00000x

www.rsc.org/

Complex Core@Shell and Core@Shell@Shell nanoparticles are systems that combine the functionalities of the inner core and outer shell materials together with new physico-chemical properties originated by their low (nano) dimensionality. Such nanoparticles are of primer importance in the fast growing nanotechnology as building blocks for more sophisticated systems and a plethora of applications. Here it is shown that, although conceptually simple, a modified gas aggregation approach allows the one-step generation of well-controlled complex nanoparticles. In particular it is demonstrated that the atoms of the core and shell of the nanoparticles can be easily inverted, avoiding intrinsic constraints of chemical methods.

Introduction

Nanoparticles (NPs) hold a special place into the nanoscience and nanotechnology not only because of their particular properties resulting from their reduced dimensions, but also because they are promising building blocks for more complex materials in nanotechnology [1]. A number of examples of NPs with new magnetic [2,3,4,5], catalytic [6,7], magneto-optical or optical [8,9,10] properties among other that differ from the bulk materials have been reported. Thanks to these new properties, NPs have been conquering increasing room in our lives and, in 2010, more than 1000 products containing nanoparticles were commercially available [11]. However, there is an increasing concern associated with the reproducible synthesis of nanomaterials [12]. Within such general frame, it appears that the development of fabrication methods of high quality NPs is a key issue to follow the increasing demand of complex multifunctional nanoparticles for advanced applications [13]. Since the initial work of Haberland et al. [14], the gas aggregation sources or Ion Cluster Sources (ICS) have been modified in many different ways. Further information on the ICS can be found in the literature [15-17]. The recent development of the Multiple Ion Cluster Source, MICS [18], open a new range of possibilities as it is possible to grow complex NPs with adjustable chemical composition and size [19]. Here, we show that the MICS represents a powerful tool to generate high quality complex NPs in one single step. In particular we show that, besides the possibility of growing alloyed NPs with controlled stoichiometry [19], the MICS can be used for the one-step generation of core@shell (CS) and core@shell@shell (CSS) nanoparticles. The proposed fabrication method allows a fine tune and control of the structure and chemical composition that will define the properties and, therefore, the functionalities of the NPs.

Experimental

The nanoparticles were grown in a MICS were the 3 magnetrons were loaded with high purity Co, Au and Ag targets [20]. The MICS was connected to an UHV chamber with base pressure in the middle 10^{-9} mbar were the NPs were deposited on TEM carbon coated grids. The magnetron efficiencies in terms of number of nanoparticles per surface area per time were determined by AFM analysis as described elsewhere [21,22]. The working parameters of each magnetron (argon flux, applied power and distance from exit slit) were adjusted in order to produce the density of ions needed to form the cores and shells of predefined dimensions. Typically the applied powers were in the range 4-10 Watt, the argon flux in the range 5-40 sccm (standard cubic centimeter per minute) and the distances of the magnetrons from the exit slit in the range 75 – 160 mm. More information regarding this new type of gas aggregation can be found in the Appendix 1. Electron microscopy measurements were performed with a FEI-TITAN X-FEG transmission electron microscope used in STEM mode and operated at 300 kV and at 120 kV. The images were acquired using a high angle annular dark field (HAADF) detector. In addition, the microscope is equipped with

monochromator, Gatan Energy Filter Tridiem 866 ERS, and a spherical aberration corrector (CEOS) for the electron probe, allowing an effective 0.08 nm spatial resolution. The column is also fitted with energy dispersive X-ray spectroscopy (EDS).

Results and discussion

The versatility of the MICS is illustrated in Figure 1, where it is shown that the combination of 3 elements (here Au, Ag and Co) is likely to lead 25 different NPs structures of interest. The combination of applied powers and positions of the magnetrons give the possibility to generate in one single step and under UHV conditions, five major types of clusters, namely α, β, χ, δ, ε, that correspond to single element NPs, homogeneously alloyed NPs with controlled stoichiometry, single core@shell NPs, complex core@shell NPS and core@shell@shell respectively (see Supporting information 1). ε NPs are composed by a core and 2 shells while NPs of type δ are formed by core (shell) resulting from the combination of the elements of 2 magnetrons and a shell (core) from the third magnetron. While the formation of single element NPs (α type) [21,22] is straightforward in gas aggregation sources and the formation of homogenously alloyed NPs (β type) using a MICS has been recently reported [19], more complex core@shell structures (χ, δ, ε types) have not been reported so far using a MICS.

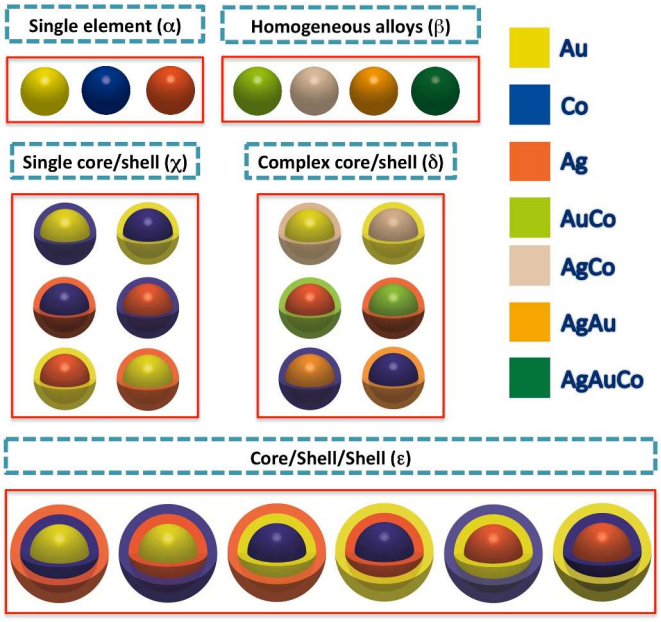

Figure 1. Illustration of the structures that can be grown using a Multiple Ion Cluster Source equipped with 3 magnetrons. Note that in the particular case given here, elements are single metal elements Au, Ag and Co. Replacing each element by complex alloys would allow the generation of more complex NPs.

Designing and tailoring core@shell NPs (CSNPs) are key issues that lead to the generation of multifunctional NPs that combine the functionalities of the individual elements into a single NP [23]. As far as we know, the combination of more than 2 elements in an aggregation zone has been reported a limited number of times in the literature [12,19,24]. Here, it is shown that χ and ε type NPs can be grown and the test elements are Co, Ag and Au. It is demonstrated that with 2 pairs of elements CSNPs can be generated in a single step using a MICS. Furthermore, it is demonstrated that inverting the positions of the magnetrons into the aggregation zone of the MICS results in the generation of the inverse CSNPs. Additionally, we show that the smart combination of 3 elements leads to the formation of a core@shell@shell structure (CSSNP) with well-defined core and 2 concentric shells.

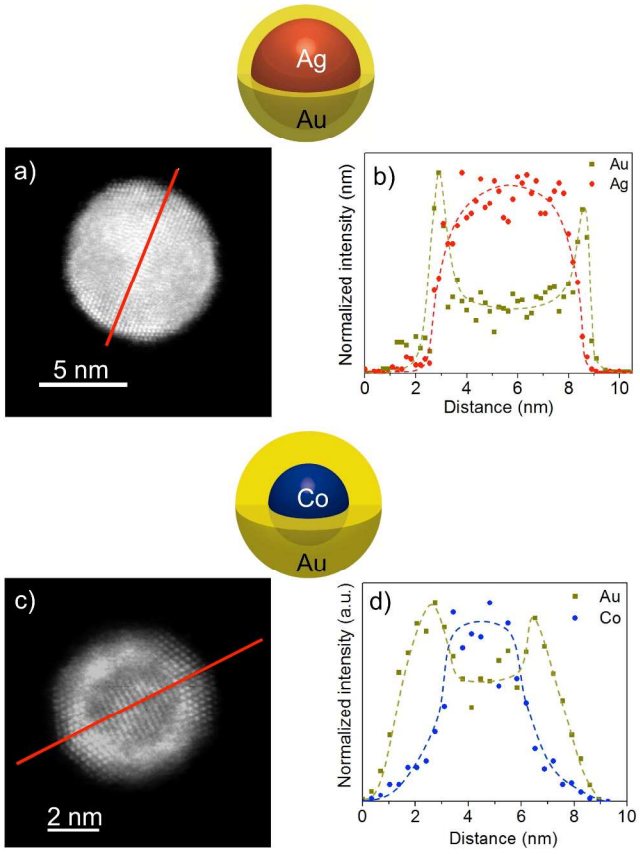

Figure 2. Core@shell Ag@Au and Co@Au nanoparticles. a) Cs-corrected STEM image of a CSNP with a core of 5.6 nm Ag and a shell of 1.2 nm Au. The brighter Au planes in the outer shell are clearly distinguished form the Ag core. b) Confirmation of the CS structure directly given by the EDS line scans performed along the line displayed in Figure 2a. c) Cs-corrected STEM image of a CSNP with a core of 3.1 nm Co and a shell of 1.4 nm Au. d) EDS line scans performed along the line displayed in Figure 2c.

Figure 2 presents a first example of CSNPs with an Ag core and an Au shell (Ag@Au) generated with the Ag magnetron placed behind the Au magnetron. The Ag seed NPs are then covered by Au in their way through the aggregation zone, resulting in the formation of an Ag@Au structure. Note that the formation of Ag@Au NPs in UHV would lead to non oxidized Ag thanks to the Au protective shell, i.e preserving the properties of Ag. Figure 2a displays a representative spherical aberration (Cs) corrected high-resolution scanning transmission electron microscopy (HRSTEM) image of an Ag@Au NP with icosahedral morphology. Although most of the NPs of the deposit presented the desired Ag@Au structure, it is worth mentioning that NPs with other structures (pure Au, pure Ag and AuAg alloy) were detected (cf. Supporting information 2). The mean size of the NPs is quite homogeneous (Figure S2.1); however if further size control is desired, they could be mass

selected by using a quadrupole mass filter (not implemented here). This observation is extensive for all the structures presented in this work. The energy dispersive x-ray spectroscopy (EDS) line scan displayed in Figure 2b clearly highlights the CS structure of the NP where the Ag atoms are confined in the core and the Au atoms surround it forming a thin shell of 1.2 nm. Note that despite the miscibility of Ag and Au, a sharp interface between both elements is observed. Another example of one-step generation of CSNPs is illustrated in Figure 2c and 2d for the case of Co core and Au shell (Co@Au). Figure 2c shows a representative Cs-corrected HRSTEM image of a Co@Au NP. In this case, the composition of the nanoparticle is even more evident just by simple observation due to the large Z difference between Au and Co. This CS structure is easily visualized in the EDS line scans displayed in Figure 2d. As general trend, the dimensions of the core and shell can be tuned through the power applied to the magnetrons, and hence the mass of the NPs can be adjusted in-situ during the fabrication of the NPs. The magnetic properties of a multilayered Co@Au NPs deposit have been investigated using a Superconducting Quantum Interference Device (SQUID) magnetometer and displayed the expected behavior (cf. Supporting information 3). In particular, the assembly of Co@Au NPs exhibited a low blocking temperature TB ≈ 3 K in agreement with the small Co magnetic core (3.1 nm diameter) and the absence of exchange bias consistent with a uniform protective Au shell.

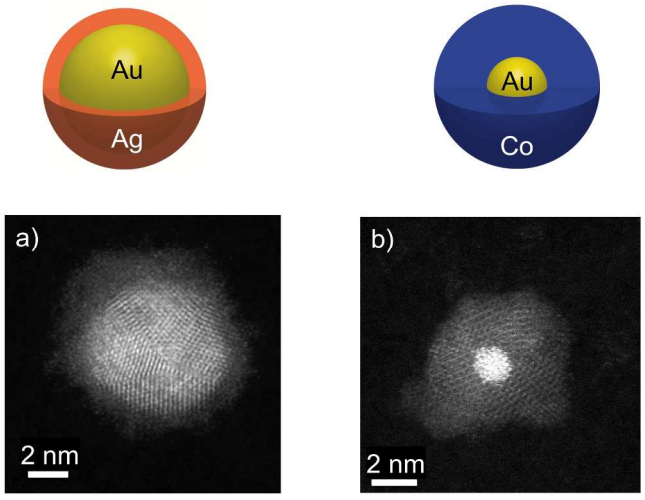

Figure 3. Core@shell Au@Ag and Au@Co nanoparticles. a) Representative Cs-corrected STEM image of a Au@Ag NP were the high crystalline nature of the Au core is distinguished adopting decahedral shape. b) representative Cs-corrected STEM image of a Au@Co NP.

As stated above, the versatility of the MICS, also resides in the ability to generate the "inverse" structures of the CSNPs presented in Figure 2. The Au@Ag and Au@Co NPs have been grown by just inverting the positions of the magnetrons inside the aggregation zone. Figure 3a displays a representative Cs-corrected HRSTEM image of the Au@Ag NPs. The crystalline Au core (with decahedral structure) appears brighter as a result of the higher scattering factor and the Ag shell is less bright due to the lower Z, where no crystalline order could be detected due to its oxidation during the sample transfer from the MICS to the TEM. Similar results on the inverse CS Au@Co structure are presented in Figure 3b. The crystalline Au core of less than 2 nm is clearly observed in the Cs-corrected HRSTEM image while the oxidized Co shell appears more crystalline than the Ag oxide, adopting the Fd-3m space group symmetry of the Co_3O_4, observed for this particular case along the [211] orientation. Note that in these inverse CSNPs, the size of the Au core as well as the shells have been modified in order to illustrate the possibility to fine tune both the core size and shell thickness of the nanoparticles.

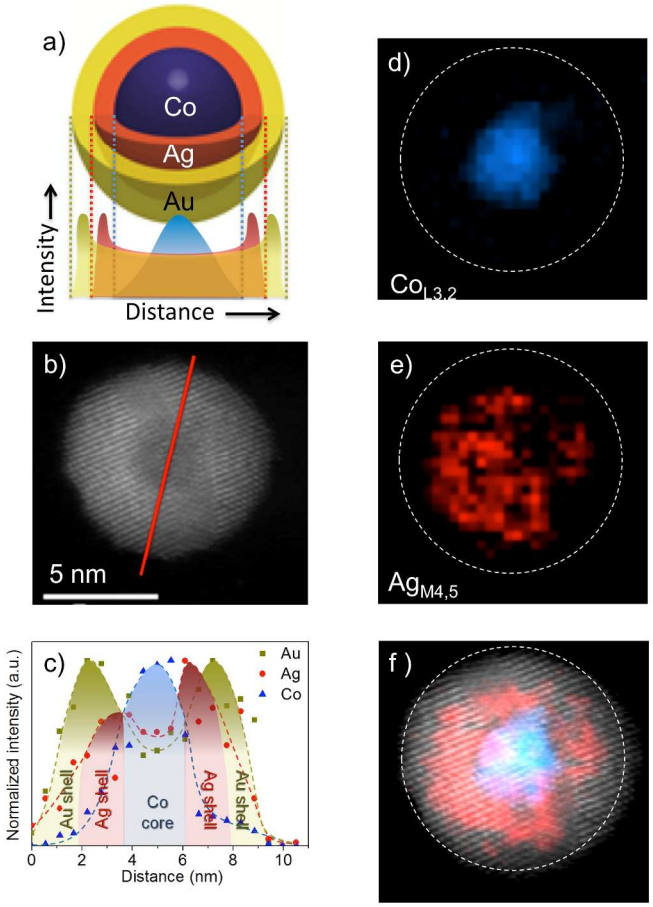

Figure 4. Core@shel@shell Co@Ag@Au nanoparticles. a) Representation of the complex Co@Ag@Au structure together with the expected EDS intensity profiles. b) Cs-corrected STEM representative image of a Co@Ag@Au NP. c) EDS line scan performed at the Co, Ag and Au, along the line depicted in Figure 4b. d) EELS compositional analysis for the Co $L_{3,2}$ edge. The dashed line represents the outer limit of the NP. e) EELS map for the Ag $M_{4,5}$ edge. f) STEM image together with the corresponding Co and Ag EELS concentration maps superimposed.

The formation of the more complex coreCo@shellAg@shellAu structure in one single step is also possible by placing, for instance, the Ag magnetron between the Co and Au magnetrons in such a way that seeds Co NPs are first covered by Ag and subsequently "protected" by Au. This is illustrated in Figure 4. Figure 4a displays the representation of the expected CSS structure and its corresponding EDS analysis profile. The experimental results are presented in Figures 4b-f. The Cs-corrected HRSTEM image is presented in Figure 4b. The darker Co core is clearly distinguished at the center of the NP. However, for a neat identification of each part of such complex structure we present the EDS line scans obtained for the Co, Ag and Au along the line depicted in figure 4b. As it can be observed in Figure 4c, the NPs present a clear Co core

surrounded by firstly an Ag shell that is secondly covered by an Au shell. The CSSNP structure is further evidenced by the EELS maps performed at the Co-$L_{3,2}$ (Figure 4d) and Ag-$M_{4,5}$ edges (Figure 4e), which merged in Figure 4f provides the spatial distribution of the elements in the NP.
.

Conclusions

In summary, an innovative method that enable the growth complex spherical core@shell and core@shell@shell nanoparticles in a one step process using a Multiple Ion Cluster Source (MICS) has been presented. The inversion of the elements that constitute the core and the shell is performed by adjusting the relative positions of the magnetrons into the aggregation zone. Furthermore, core size and shell thickness can be tuned at the nanometric scale. Our proof-of-concept demonstrates that it is possible to growth high purity NPs with complex structures for future applications and also to use the MICS as a tool for the study of fundamental properties of novel nanoparticles.

Acknowledgements

Work was supported by the Spanish Ministerio de Ciencia e Innovación under projects MAT2008-06765-C02, MAT2011-29194-C02-02, MAT2011-27470-C02-02, CSD2007-00041 (NANOSELECT), and CSD2009-00013 (IMAGINE). D. Llamosa P. acknowledges financial support from Ministerio de Ciencia e Innovación under contract n° JAEPre-09-01925. M.R. acknowledges the FPI grant from the Spanish Ministerio de Economía y Competitividad. L. M. and E. R. acknowledge the Consejo Superior de Investigaciones Cientifícas (PIE 201160E085). The microscopy works have been conducted in the Laboratorio de Microscopias Avanzadas at Instituto de Nanociencia de Aragon - Universidad de Zaragoza, Spain.

Notes and references

[a] Instituto de Ciencia de Materiales de Madrid, Consejo Superior de Investigaciones Científicas (CSIC), C/Sor Juana Inés de la Cruz, 3, 28049 Madrid, Spain.

[b] Laboratorio de Microscopías Avanzadas (LMA), Instituto de Nanociencia de Aragón (INA), Universidad de Zaragoza, c/Mariano Esquillor, Edificio I+D, 50018 Zaragoza, Spain.

Electronic Supplementary Information (ESI) available:

Supporting Information 1: scheme illustrating the different strategies to grow nanoparticles with controlled chemical composition and structure.

Supporting Information 2: examples of TEM results on Ag@Au nanoparticles.

Supporting Information 3: magnetic measurements results on Co@Au and Au@Co nanoparticles.

1 U. Simon, *Nature Materials*, 2013, **12**, 694.

2 B. Sampedro, P. Crespo, A. Hernando, R. Litrán, J. C. Sánchez López, C. López Cartes, A. Fernandez, J. Ramírez, J. González Calbet and M. Vallet. *Phys. Rev. Lett.*, 2003, **91**, 237203.

3 I. M. L. Billas, J. A. Becker, A. Châtelain and Walt A. de Heer, *Phys. Rev. Lett.*, 1993, **71**, 4067

4 X. Wan, L. Zhou, J. Dong, T. K. Lee and Ding-sheng Wang, *Phys. Rev. B.*, 2004, **69**, 174414.

5 V. Skumryev, S. Stoyanov, Y. Zhang, G. Hadjipanayis, D. Givord and J. Nogues, *Nature*, 2003, **423**, 850.

6 M. Valden, X. Lai and D. W. Goodman, *Science*, 1998, **281**, 1647.

7 K. Mori and H. Yamashita, *Phys. Chem. Chem. Phys.*, 2010, **43**, 14420.

8 S. Serrano-Guisan, G. Di Domenicantonio, M. Abid, J. P. Abid, M. Hillenkamp, L. Gravier, J. P. Ansermet and C. Felix, *Nature Materials*, 2006, **5**, 730.

9 G. E. Jonsson, H. Fredriksson, R. Sellappan and D. Chakarov, *International Journal of Photoenergy*, 2011, Article ID 939807

10 V. Myroshnychenko, J. Rodríguez-Fernández, I. Pastoriza-Santos, A. M. Funston, C. Novo, P. Mulvaney, L. M. Liz-Marzán and F. J. García de Abajo, *Chem. Soc. Rev.*, 2008, **37**, 1792.

11 C. Ostiguy, B. Roberge, C. Woods and B. Soucy, Engineered Nanoparticles Current Knowledge about OHS Risks and Prevention Measures, Second Edition, Studies and Research Projects, Report 656, Institut de recherche Robert-Sauvé en santé et en sécurité du travail (IRSST), 2010.

12 D. R. Baer, M. H. Engelhard, G. E. Johnson, J. Laskin, J. Lai, K. Mueller, P. Munusamy, S. Thevuthasan, H. Wang, N. Washton, A. Elder, B. L. Baisch, A. Karakoti, S. V. N. T. Kuchibhatla and D. W. Moon, *J. Vac. Sci. Technol. A*, 2013, **31**, 050820.

13 E. R. Zubarev, *Nature Nanotechnology*, 2013, **8**, 396.

14 H. Haberland, M. Karrais and M. Mall, *Z. Phys. D: At., Mol. Clusters*, 1991, **20**, 413.

15 C. Xirouchaki and R. E. Palmer, *Philos. Trans. R. Soc., A*, 2004, **362**, 117.

16 K. Wegner, P. Piseri, H. Vahedi Tafreshi and P. Milani, *J. Phys. D: Appl. Phys.*, 2006, **39**, R439.

17 A. Perez, P. Mélinon, V. Dupuis, L. Bardotti, B. Masenelli, F. Tournus, B. Prével, J. Tuaillon-Combes, E. Bernstein, A. Tamion, N. Blanc, D. Taïnoff, O. Boisron, G. Guiraud, M. Broyer, M. Pellarin, N. Del Fatti, F. Vallée, E. Cottancin, J. Lermé, J. L. Vialle, C. Bonnet, P. Maioli, A. Crut, C. Clavier, J. L. Rousset and F. Morfin, *Int. J. Nanotechnol.*, 2010, **7**, 523.

18 E. L. Román García, L. Martínez Orellana, M. Díaz Lagos, Y. Huttel, Spanish Patent P201030059, 2010.

19 L. Martínez, M. Díaz, E. Román, M. Ruano, D. Llamosa P. and Y. Huttel, *Langmuir*, 2012, **28**, 11241.

20 Oxford Applied Research Ltd., www.oaresearch.co.uk

21 M. Ruano, L. Martínez and Y. Huttel, *Dataset Papers in Science*, 2013, Article ID 597023.

22 D. Llamosa P., L. Martínez and Y. Huttel, Y. Dataset Papers in Science, Nanotechnology, 2014, Article ID 584391.

23 S. Peng, C. Lei, Y. Ren, R. E. Cook and Y. Sun, *Angew. Chem. Int. Ed.*, 2011, **50**, 3158.

24 M. Benelmekki, M. Bohra, Jeong-Hwan Kim, R. E. Diaz, J. Vernieres, P. Grammatikopoulos and M. Sowwan, *Nanoscale*, 2014, **6**, 3532.

